Reactions of the Electron-Rich Binuclear Hydride Complexes $[\{Pr^i_2P(CH_2)_xPPr^i_2\}Rh]_2(\mu\text{-}H)_2$ (x = 2 or 3) with ZnR_2 and MgR'_2

Michael D. Fryzuk,*,† David H. McConville,‡ and Steven J. Rettig§

Department of Chemistry, University of British Columbia, 2036 Main Mall, Vancouver, BC, Canada V6T 1Z1

Received July 21, 1992

The reaction of dialkylzinc reagents (ZnR_2; R = CH_2Ph, C_5H_5, C_3H_5) with the binuclear hydride dimers $[P_2Rh]_2(\mu\text{-}H)_2$ (P_2 = dippp = 1,3-bis(diisopropylphosphino)propane, dippe = 1,2-bis(diisopropylphosphino)ethane) yields two products: the first is a mononuclear Rh(I) derivative P_2RhR and the second is a tetranuclear complex of the general formula $[P_2Rh]_2(\mu\text{-}H)_2(\mu\text{-}ZnR)_2$. Two of the tetranuclear species have been studied crystallographically. The molecular structure of $[(dippp)Rh]_2(\mu\text{-}H)_2(\mu\text{-}ZnCH_2Ph)_2$ (a = 19.608(7) Å, b = 12.891(6) Å, c = 22.847(6) Å, β = 120.02(2)°, Z = 4, fw = 1073.61, ρ(calcd) = 1.426 g cm^{-3}, space group = $C2/c$) reveals a dirhodium core symmetrically bridged by two hydrides and two $ZnCH_2Ph$ units. The molecular structure of $[(dippp)Rh]_2(\mu\text{-}H)_2(\mu\text{-}ZnC_5H_5)_2\cdot CH_3C_6H_5$ (a = 12.050(6) Å, b = 35.230(4) Å, c = 12.414(2) Å, β = 97.84(3)°, Z = 4, fw = 1113.68, ρ(calcd) = 1.417 g cm^{-3}, space group = $P2_1/n$) also shows a dirhodium core, but in this case, there are two unsymmetrically bridging ZnC_5H_5 units, one hydride which bridges the two rhodium centers and one hydride which bridges a rhodium and a ZnC_5H_5 unit. The reaction of dibenzylmagnesium with $[(dippp)Rh]_2(\mu\text{-}H)_2$ is similar in that the Rh(I) species $(dippp)Rh(\eta^3\text{-}CH_2Ph)$ is formed; however, the second product is believed to be the heterobimetallic complex $P_2RhH_2MgCH_2Ph$ that does not dimerize. The Rh–Zn complexes react reversibly with dihydrogen to give binuclear polyhydrides that are in equilibrium with monomeric Rh(III) complexes of the form P_2RhH_2ZnR. The Rh–Mg complex reacts reversibly with dihydrogen to give a heterobinuclear tetrahydride. Mechanistic studies are presented that show the formation of the Rh–Zn tetranuclear species involves fragmentation followed by recombination steps.

Introduction

Ternary metal hydrides, having the general formula $A_xM_yH_z$ (A = electropositive metal; M = transition or lanthanide metal), constitute a class of materials that are of interest for their magnetic, electrical, and bonding properties[1] as well as their potential for hydrogen storage systems.[2] The preparation of these solid-state materials is not straightforward, often relying on serendipity for the production of particular stable phases.[1] In addition, determining structures and properties of these materials can be hampered by the fact that they are sometimes amorphous and/or nonstoichiometric in nature.[3] In an effort to model such materials we have been examining soluble, hydrogen-rich, molecular hydride complexes containing rhodium and some electropositive metal such as magnesium or zinc. Our goals are to prepare heterobimetallic clusters that are soluble, well-defined complexes and examine their structures and their reactivity particularly with hydrogen.

Scheme I

$$L_xMH + ZnR_2 \xrightarrow{-RH} L_xM\text{-}ZnR$$

$$L_xM\text{-}ZnR \rightleftharpoons {}^1/_2ZnR_2 + {}^1/_2[L_xM]_2Zn$$

The literature indicates that compounds that contain a direct transition metal-to-zinc bond have been known for some time;[4–6] they include zinc–bis(transition metal) compounds (e.g. $Zn[Co(CO)_4]_2$[7]), transition metal–zinc halides (e.g., $(OC)_4Fe(ZnCl)_2$[8]), organozinc–transition metal compounds (e.g. $CpZnMn(CO)_5$[9]), and cluster complexes such as $Cp_6Ni_2Zn_4$.[10] One of the methods[11] used to generate transition metal–zinc bonds is the reaction of a transition metal hydride with a dialkylzinc derivative via elimination of hydrocarbon to give the unsymmetrical product $L_xM\text{-}ZnR$ (Scheme I). The equilibrium between the unsymmetrical complex $L_xM\text{-}ZnR$ and the symmetric products of disproportionation[12] ZnR_2 and $[L_xM]_2Zn$ usually lies so far to the right that the intermediate $L_xM\text{-}ZnR$ species cannot be isolated. However, the equilibrium can be shifted to the left by employing polyhaptic[9] ligands, such as cyclopentadienyl, that can provide coordinative saturation to the zinc atom. For example, the reaction of Cp_2NbH_3 with $ZnEt_2$[13] leads to the formation of the sym-

---

† E. W. R. Steacie Fellow (1990–1992).

‡ NSERC Graduate Scholarship (1989–1991).

§ Experimental Officer, UBC Crystal Structure Service.

(1) Bronger, W. *Angew. Chem., Int. Ed. Engl.* 1991, *30*, 759.

(2) Bogdanovic, B.; Ritter, A.; Spliethoff, B. *Angew. Chem., Int. Ed. Engl.* 1990, *29*, 223.

(3) Nesper, R. *Angew. Chem., Int. Ed. Engl.* 1991, *30*, 789.

(4) Burlitch, J. M. *J. Chem. Soc., Chem. Commun.* 1968, 887.

(5) Carey, N. A. D.; Noltes, J. G. *J. Chem. Soc., Chem. Commun.* 1968, 7471.

(6) Francis, B. R.; Green, M. L. H.; Luong-thi, T.; Moser, G. A. *J. Chem. Soc., Dalton Trans.* 1977, 1339.

(7) Heiber, W.; Teller, U. *Anorg. Allg. Chem.* 1942, *249*, 43.

(8) Burlitch, J. M.; Winterton, R. C. *Inorg. Chem.* 1979, *18*, 2309.

(9) Budzelaar, P. H. M.; Boersma, J.; van der Kerk, G. J. M. *J. Organomet. Chem.* 1980, *202*, C71.

(10) Budzelaar, P. H. M.; Boersma, J.; van der Kerk, G. J. M. *Angew. Chem.* 1983, *95*, 335.

(11) St. Denis, J. N.; Butler, W.; Glick, M. D.; Oliver, J. P. *J. Organomet. Chem.* 1977, *129*, 1.

(12) Budzelaar, P. H. M.; Alberts-Jansen, H. J.; Mollema, K.; Boersma, J.; van der Kerk, G. J. M.; Spek, A. L.; Duisenberg, A. J. M. *J. Organomet. Chem.* 1983, *243*, 137.

0276-7333/93/2312-2152$04.00/0

metrical trinuclear species $[Cp_2NbH_2]_2Zn$ whereas the reaction of the same niobium complex with $ZnCp_2$[14] generates the binuclear, unsymmetrical derivative $Cp_2NbH_2(ZnCp)$.

In comparison to zinc, the number of known transition metal–magnesium-bonded species is small.[15–18] The magnesium atom in the iron complex $CpFe(dppe)MgBr(THF)_2$ is tetrahedrally coordinated with an iron–magnesium bond length of 2.593(7) Å.[15] Analogous elimination reactions to those depicted in Scheme I have not been reported for diorganomagnesium reagents.

In this paper we describe the reactivity of electron-rich, coordinatively unsaturated rhodium hydride dimers $[\{Pr^i_2P(CH_2)_xPPr^i_2\}Rh]_2(\mu\text{-}H)_2$ (I, x = 3; II, x = 2)[19–21] toward dialkylzinc and dialkylmagnesium reagents. In the former set of reactions, unusual tetranuclear clusters are obtained in a series of fragmentation–recombination reactions,[22] while in the latter, monomeric bimetallic species are obtained. These new materials show reversible hydrogen uptake under mild conditions.

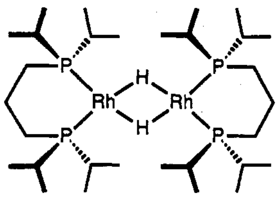

I $[(dippp)Rh]_2(\mu\text{-}H)_2$

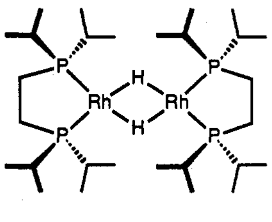

II $[(dippe)Rh]_2(\mu\text{-}H)_2$

Results and Discussion

Reactions with $Zn(CH_2Ph)_2$. The reaction of $[(dippp)Rh]_2(\mu\text{-}H)_2$ (I) with 1 equiv of dibenzylzinc, $Zn(CH_2Ph)_2$,[23] in toluene did not lead to the expected symmetrical complex $[(dippp)Rh]_2Zn$, by elimination of 2 equiv of toluene, but rather gave two products in a 1:1 ratio, as determined by $^{31}P\{^1H\}$ NMR spectroscopy (eq 1). The

$$\begin{gathered}[P_2Rh]_2(\mu\text{-H})_2 + Zn(CH_2Ph)_2 \xrightarrow{-{}^1/_2H_2} \\ {}^1/_2[P_2Rh]_2(\mu\text{-H})_2(\mu\text{-ZnCH}_2\text{Ph})_2 + \\ \mathbf{1a}, P_2 = \text{dippp} \\ \mathbf{1b}, P_2 = \text{dippe} \\ P_2Rh(\eta^3\text{-CH}_2\text{Ph}) \quad (1) \\ \mathbf{2a}, P_2 = \text{dippp} \\ \mathbf{2b}, P_2 = \text{dippe}\end{gathered}$$

two compounds could be separated by fractional crystallization from toluene at −40 °C. The more soluble complex was identified as the mononuclear η^3-benzyl derivative $(dippp)Rh(\eta^3\text{-}CH_2Ph)$ (**2a**); in fact, **2b** can be synthesized directly from $[(dippp)Rh]_2(\mu\text{-}Cl)_2$[20] and a variety of benzylating reagents.[24] The less soluble derivative, **1a**, was shown to be a tetranuclear derivative, as discussed below. The analogous reaction with the rhodium dippe hydride dimer (II) yields compounds **1b** and **2b**, respectively, in quantitative yield.

The ^1H NMR spectra of the less soluble components **1a** and **1b** show a singlet for the benzylic protons (CH_2Ph) and a multiplet for the hydrides in the ratio of 2:1 with respect to a single diphosphine ligand; an initial empirical formula of $P_2RhH(ZnCH_2Ph)$ for each of **1a** (P_2 = dippp) and **1b** (P_2 = dippe) also agrees with the analytical data. However, the hydride multiplets were in fact a quintet of triplets due to coupling to four equivalent phosphorus-31 and two equivalent rhodium-103 nuclei; therefore, the structures of both **1a** and **1b** are tetranuclear in solution; that is, the molecular formula of these species is of a dimeric, bimetallic complex, $[P_2RhH(ZnCH_2Ph)]_2$. Further evidence for the dimeric structures of these complexes is observed in the $^{31}P\{^1H\}$ NMR spectra which show a symmetrical doublet of multiplets resonance normally associated with binuclear rhodium diphosphine complexes bearing chemically equivalent yet magnetically inequivalent phosphine donors.[19–21,36] The diphosphine ligand region in the ^1H NMR spectra of **1a** and **1b** displays one isopropyl methine and two isopropyl methyl resonances, indicating a symmetric environment above and below the plane of the coordinated ligand. An X-ray crystallographic analysis of **1a** was undertaken in order to determine its structure and the nature of the bonding in the complex.

Molecular Structure of $[(dippp)Rh]_2(\mu\text{-}H)_2(\mu\text{-}ZnCH_2Ph)_2$, 1a. The molecular structure of $[(dippp)Rh]_2(\mu\text{-}H)_2(\mu\text{-}ZnCH_2Ph)_2$, **1a**, is shown in Figure 1 (bond lengths and angles appear in Table III). The dimeric structure consists of two (dippp)Rh fragments bridged symmetrically by two $ZnCH_2Ph$ units and two hydrides, the latter of which were located in the final difference Fourier map. Removal of the ancillary ligands from the tetranuclear complex (bridging hydrides and diphosphines) reveals a distorted tetrahedral arrangement of the two rhodium and two zinc atoms (Figure 2a). The Zn–Zn separation of 3.015 Å is rather long to invoke a formal Zn–Zn single bond. A similar tetrahedral arrangement of two cobalt and two zinc atoms has been observed in the solid-state structure[25] of $[(OC)_3Co]_2(\mu\text{-}CO)(\mu\text{-}ZnCo(CO)_4)$

---

[13] Tebbe, F. N. *J. Am. Chem. Soc.* **1973**, *95*, 5412.

[14] Budzelaar, P. H. M.; den Haan, K. H.; Boersma, J.; van der Kerk, G. J. M.; Spek, A. L. *Organometallics* **1984**, *3*, 156.

[15] Felkin, H.; Knowles, P. J.; Meunier, B.; Mitschler, A.; Picard, L.; Weiss, R. *J. Chem. Soc., Chem. Commun.* **1974**, 44.

[16] Prout, K.; Forder, R. A. *Acta Crystallogr.* **1975**, *B31*, 852.

[17] Davies, S. G.; Green, M. L. H. *J. Chem. Soc., Dalton Trans.* **1978**, 1510.

[18] Jonas, K.; Koepe, G.; Krueger, C. *Angew. Chem.* **1986**, *98*, 901.

[19] Fryzuk, M. D.; Piers, W. E. *Polyhedron* **1988**, *7*, 1001.

[20] Fryzuk, M. D.; Piers, W. E.; Rettig, S. J.; Einstein, F. W. B.; Jones, T.; Albright, T. A. *J. Am. Chem. Soc.* **1989**, *111*, 5709.

[21] Fryzuk, M. D.; Rosenberg, L.; Rettig, S. J. *Organometallics* **1991**, *10*, 2537.

[22] Fryzuk, M. D.; McConville, D. H.; Rettig, S. J. *Organometallics* **1990**, *9*, 1359.

[23] Schrock, R. R. *J. Organomet. Chem.* **1976**, *122*, 209.

[24] Fryzuk, M. D.; McConville, D. H.; Rettig, S. J. *J. Organomet. Chem.* **1993**, *445*, 245.

[25] Burlitch, J. M.; Hayes, S. E.; Lemley, J. T. *Organometallics* **1985**, *4*, 167.

[26] Fischer, B. Ph.D. Thesis, Rijksuniversiteit van Utrecht, 1989.

[27] Budzelaar, P. H. M.; Boersma, J.; van der Kerk, G. J. M.; Spek, A. L.; Duisenberg, A. J. M. *Inorg. Chem.* **1982**, *21*, 3777.

[28] Porai-Koshits, A. A.; Antsyshkina, A. S.; Pasynskii, A. A.; Sadikov, G. G.; Skripkin, Y. V.; Ostrikova, A. N. *Inorg. Chim. Acta* **1979**, *34*, L285.

[29] Bansemer, R. L.; Huffman, J. C.; Caulton, K. G. *J. Am. Chem. Soc.* **1983**, *105*, 6163.

[30] Han, R.; Gorrell, I. B.; Looney, A.; Parkin, G. *J. Chem. Soc., Chem. Commun.* **1991**, 717.

[31] Fischer, B.; Boersma, J.; van Koten, G.; Spek, A. L. *New J. Chem.* **1988**, *12*, 613.

[32] Cummings, C. C.; Schrock, R. R.; Davis, W. M. *Organometallics* **1991**, *10*, 3781.

[33] Brown, H. C.; Racherla, U. S. *J. Org. Chem.* **1986**, *51*, 427.

[34] Fryzuk, M. D.; Piers, W. E.; Einstein, F. W. B.; Jones, T. *Can. J. Chem.* **1989**, *67*, 883.

[35] Piers, W. E. Ph.D. Thesis, The University of British Columbia, 1988.

[36] Nixon, J. F.; Pidcock, A. *Annu. Rev. NMR Spectrosc.* **1969**, *2*, 345.

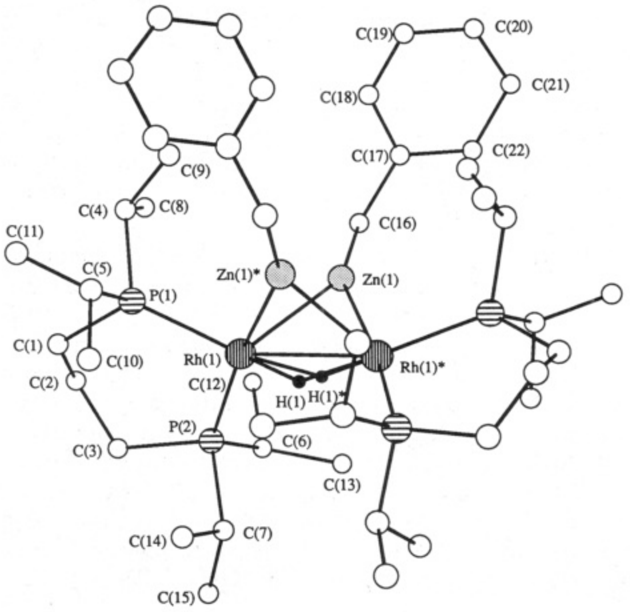

Figure 1. Molecular structure and numbering scheme for $[(\mathrm{dippp})\mathrm{Rh}]_2(\mu\text{-H})_2(\mu\text{-ZnCH}_2\mathrm{Ph})_2$ (**1a**).

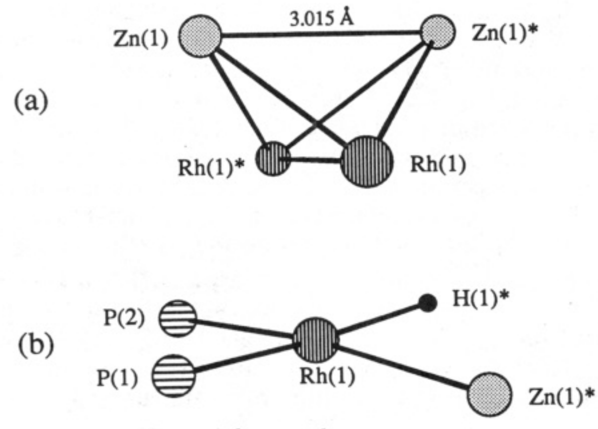

Figure 2. (a) View of the metal core of **1a**. (b) View of the square-planar arrangement of atoms about rhodium.

(III); in this case the zinc atoms are separated by 3.568 Å and this certainly precludes any significant Zn–Zn bonding.

A second feature of the solid-state structure of the tetranuclear complex $[(\mathrm{dippp})\mathrm{Rh}]_2(\mu\text{-H})_2(\mu\text{-ZnCH}_2\mathrm{Ph})_2$, **1a**, is the coordination geometry of the ligands around each rhodium center. The donor atoms of the diphosphine, one of the bridging hydrides, and one of the bridging zinc benzyl moieties form a nearly perfect square plane about the rhodium center (Figure 2b). Therefore, the dimer can be viewed as two interlocked square planar rhodium units, $(\mathrm{dippp})\mathrm{RhH}(\mathrm{ZnCH}_2\mathrm{Ph})$, which are separated by a Rh–Rh distance of 2.764 Å, which is well within range to invoke a single bond.

Reaction with $\mathbf{Zn(C_5H_5)_2}$. In an effort to study the generality of the above reaction other dialkylzinc reagents were employed. The reaction of 1 equiv of bis(cyclopentadienyl)zinc, $\mathrm{Zn}(C_5H_5)_2$,[26] with the hydride dimer $[(\mathrm{dippp})\mathrm{Rh}]_2(\mu\text{-H})_2$, I, in toluene or THF yields the tetranuclear complex $[(\mathrm{dippp})\mathrm{Rh}]_2(\mu\text{-H})_2(\mu\text{-ZnC}_5\mathrm{H}_5)_2$ (**1c**) and the mononuclear derivative $(\mathrm{dippp})\mathrm{Rh}(\eta^5\text{-}C_5H_5)$ (**2c**) quantitatively, as determined by $^{31}\mathrm{P}\{^1\mathrm{H}\}$ NMR spectroscopy (eq 2). The tetranuclear complex **1c** could be obtained as orange crystals in high yield (88%) by cooling (−40 °C) a toluene solution containing a mixture of compounds **1c** and **2c**. While the derivative **2c** could not be separated from compound **1c** easily, it has been prepared in quantitative yield by reacting $\mathrm{Zn}(C_5H_5)_2$ with $[(\mathrm{dippp})\mathrm{Rh}]_2(\mu\text{-Cl})_2$.[20]

$$[(\mathrm{dippp})\mathrm{Rh}]_2(\mu\text{-H})_2 + \mathrm{Zn}(C_5H_5)_2 \xrightarrow{-{}^1/_2\mathrm{H}_2} {}^1/_2\underset{\mathbf{1c}}{[(\mathrm{dippp})\mathrm{Rh}]_2(\mu\text{-H})_2(\mu\text{-ZnC}_5\mathrm{H}_5)_2} + \underset{\mathbf{2c}}{(\mathrm{dippp})\mathrm{Rh}(\eta^5\text{-}C_5H_5)} \quad (2)$$

The ^{1}H NMR spectrum of complex **1c** shows a singlet for the Cp group at 6.48 ppm, which is close to the chemical shift for the free cyclopentadienyl anion.[27] A symmetrical septet is seen at −12.12 ppm, which has been assigned as two bridging hydrides with equal coupling to two ^{103}Rh nuclei and four ^{31}P nuclei, suggesting that compound **1c** is similar to the tetranuclear zinc benzyl complex **1a** in solution. A single resonance is seen for the isopropyl methines, and two resonances are observed for the isopropyl methyls, indicating a high degree of symmetry in the complex in solution. The temperature invariant $^{31}\mathrm{P}\{^1\mathrm{H}\}$ NMR spectrum of compound **1c** shows a symmetric doublet of multiplets centered at 44.7 ppm with a coupling to ^{103}Rh of 151 Hz. The coupling to rhodium and the location of the doublet pattern is very close to that observed for $[(\mathrm{dippp})\mathrm{Rh}]_2(\mu\text{-H})_2(\mu\text{-ZnCH}_2\mathrm{Ph})_2$, **1a**.

Molecular Structure of $\mathbf{[(dippp)Rh]_2(\mu\text{-}H)_2(\mu\text{-}ZnC_5H_5)_2}$, 1c. The molecular structure of $[(\mathrm{dippp})\mathrm{Rh}]_2(\mu\text{-H})_2(\mu\text{-ZnC}_5\mathrm{H}_5)_2$, **1c**, is shown in Figure 3; bond lengths and angles appear in Table V. The structure of complex **1c** consists of two (dippp)Rh fragments bridged unsymmetrically by two ZnCp units and one hydride. The rather large Rh–Rh separation of 2.9507(9) Å and the significantly closer approach (~0.13 Å) of the two zinc atoms to Rh(2) than to Rh(1) would seem to suggest that a Rh(I)–Rh(III) formalism is in order. Unexpectedly, a second hydride was found to occupy a bridging position between Zn(2) and Rh(1). There are relatively few examples of structurally characterized complexes which bear hydrides bound directly to zinc.[28–30]

The degree of asymmetry in the tetranuclear complex is undoubtedly due to the presence of the second hydride which bridges Zn(2) and Rh(1) (Figure 4). Inspection of the coordination sphere of Rh(2) reveals a nearly square planar arrangement of two phosphines (P(3) and P(4)), a hydride (H(1)) and a ZnCp unit (Zn(1)), as seen in the molecular structure of $[(\mathrm{dippp})\mathrm{Rh}]_2(\mu\text{-H})_2(\mu\text{-ZnCH}_2\mathrm{Ph})_2$, **1a**. The other rhodium atom (Rh(1)) has a different coordination geometry, with one of the phosphines (P(2)) nearly trans (171.3°) to the hydride (H(2)) which bridges Zn(2) and Rh(1). The second phosphine (P(1)) is essentially trans (157.0°) to the hydride (H(1)) which bridges the two rhodium centers.

The two cyclopentadienyl groups in $[(\mathrm{dippp})\mathrm{Rh}]_2(\mu\text{-H})_2(\mu\text{-ZnC}_5\mathrm{H}_5)_2$, **1c**, are bound in a pseudo η^3 fashion with one short and two long contacts between the zinc and the carbon atoms. Distortions of a cyclopentadienyl fragment bound to a group 12 metal are well documented.[26,31,32] The hexanuclear nickel–zinc complex $\mathrm{Zn}_4\mathrm{Ni}_2(C_5H_4R)_6$ (IV) (R = SiMe$_3$) contains cyclopentadienyl groups bound in an η^1, η^3, and η^5 fashion. The extent of the cyclopentadienyl distortion is measured by the *ring slippage* which is defined as the distance between the ring centroid and the perpendicular projection of the metal atom on the least-squares ring plane.[26,31] In complex IV the η^1-bonded

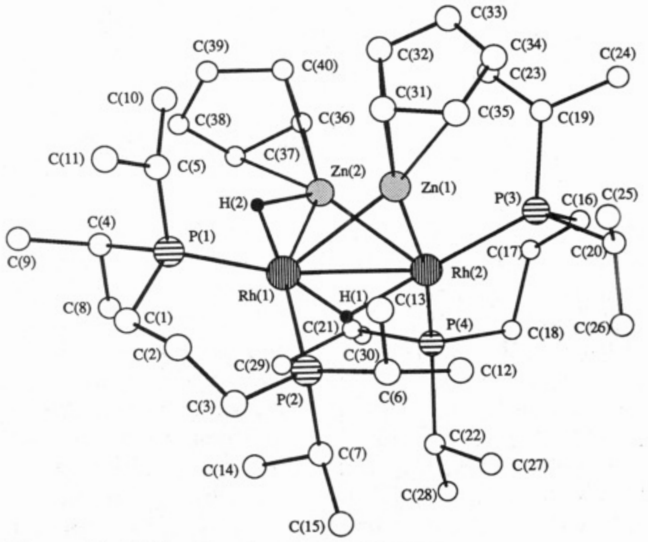

Figure 3. Molecular structure and numbering scheme for $[(dippp)Rh]_2(\mu\text{-}H)_2(\mu\text{-}ZnC_5H_5)_2$ (**1c**).

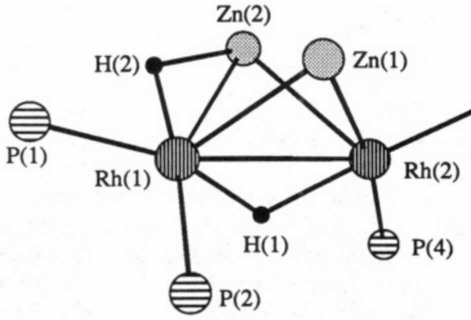

Figure 4. View of the core of **1c**.

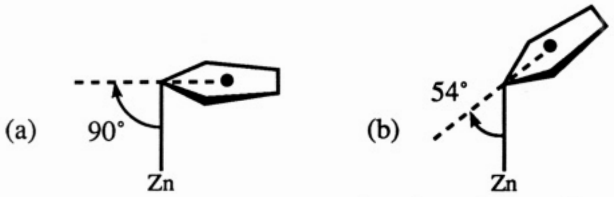

Figure 5. (a) Mainly ionic interaction of a cyclopentadienyl group with zinc. (b) Mainly covalent interaction of a cyclopentadienyl group with zinc.

cyclopentadienyl groups show a large ring slippage of 1.88 Å, while the η^3-bonded cyclopentadienyl groups show a smaller slippage of 0.72 Å. In $[(dippp)Rh]_2(\mu\text{-}H)_2(\mu\text{-}ZnC_5H_5)_2$, **1c**, the ring slippage for the cyclopentadienyl group bound to Zn(1) is 1.56 Å while that for Zn(2) is only 1.22 Å. These values fall roughly midway between the η^1 and η^3 bonding values.

The degree of covalency[26] between the cyclopentadienyl group and zinc is reflected in the angle generated by the centroid of the Cp group, the nearest carbon, and the zinc, as shown in Figure 5. An interaction between zinc and the cyclopentadienyl ligand that is characterized as being mainly ionic is manifested by a 90° angle between the least-squares plane of the Cp and the zinc and by statistically equal carbon–carbon bond lengths (Figure 5a). A mainly covalent interaction results in an angle of 54° between the least-squares plane of the Cp group and the zinc with well-defined alternating long–short carbon–carbon bond lengths which differ by ~0.15 Å throughout the Cp unit. The cyclopentadienyl group bound to Zn(1) in $[(dippp)Rh]_2(\mu\text{-}H)_2(\mu\text{-}ZnC_5H_5)_2$, **1c**, forms an angle of 80.0°, while the bond lengths in the Cp unit differ by only ~0.04 Å (i.e. statistically the same, well within 3σ). The cyclopentadienyl group attached to Zn(2) displays an angle of 89.4°, and again the carbon–carbon bond lengths in the Cp group differ by only ~0.04 Å. On the basis of the above analysis, the cyclopentadienyl ligands in $[(dippp)Rh]_2(\mu\text{-}H)_2(\mu\text{-}ZnC_5H_5)_2$, **1c**, are bound in a mainly ionic fashion. This conclusion is supported by the downfield shift of the Cp group in the ^{1}H NMR spectrum of complex **1c**.

Reaction with $Zn(C_3H_5)_2$. The reaction of 1 equiv of diallylzinc, $Zn(C_3H_5)_2$,[33] with $[(dippp)Rh]_2(\mu\text{-}H)_2$, I, in toluene or THF yields the analogous tetranuclear complex $[(dippp)Rh]_2(\mu\text{-}H)_2(\mu\text{-}ZnC_3H_5)_2$ (**1d**) and mononuclear derivative $(dippp)Rh(\eta^3\text{-}C_3H_5)$ (**2d**) in quantitative yield by $^{31}P\{^1H\}$ NMR spectroscopy (eq 3). The presence of complex **2d** was confirmed spectroscopically by comparison to an authentic sample.[34]

$$[(dippp)Rh]_2(\mu\text{-}H)_2 + Zn(C_3H_5)_2 \xrightarrow{-^1/_2H_2} \underset{\mathbf{1d}}{^1/_2[(dippp)Rh]_2(\mu\text{-}H)_2(\mu\text{-}ZnC_3H_5)_2} + \underset{\mathbf{2d}}{(dippp)Rh(\eta^3\text{-}C_3H_5)} \quad (3)$$

The $^{31}P\{^1H\}$ NMR spectrum of **1d** shows a complex doublet pattern at 47.4 ppm ($^1J_{P,Rh}$ = 155 Hz) which is comparable to the $^{31}P\{^1H\}$ NMR data of complexes **1a–c**. The ^{1}H NMR spectrum of compound **1d** shows the typical quintet of triplets resonance for the hydrides at −9.34 ppm; the allyl group is undergoing a rapid exchange of syn and anti protons, as evidenced by the quintet pattern for the central proton. Complex **1d** is assumed to be structurally similar to complexes **1a–c**. The tetranuclear complex, **1d**, could not be separated from $(dippp)Rh(\eta^3\text{-}C_3H_5)$, **2d**, due to the similar solubilities of the two species; attempts to sublime away **1d** from **2d** resulted in decomposition.

Fluxional Behavior of $[(dippp)Rh]_2(\mu\text{-}H)_2(\mu\text{-}ZnR)_2$. The ^{1}H and $^{31}P\{^1H\}$ NMR spectra of complexes **1a–d** are temperature invariant down to −80 °C. The coordination geometry about each rhodium in the solid-state structure of $[(dippp)Rh]_2(\mu\text{-}H)_2(\mu\text{-}ZnCH_2Ph)_2$, **1a**, shows clearly that the phosphorus donors of each ligand are inequivalent, one being trans to a zinc benzyl moiety and the other trans to the bridging hydride (Figure 2b). Furthermore, the chemical environment above and below the plane of the chelated diphosphine ligand is different, with a zinc benzyl moiety above and a bridging hydride below. As for the molecular structure of the tetranuclear derivative $[(dippp)Rh]_2(\mu\text{-}H)_2(\mu\text{-}ZnC_5H_5)_2$, **1c**, all four phosphine donors are inequivalent in the solid state owing to the distortion imparted by the hydride which bridges Zn(2) and Rh(1) (Figure 4). Yet the resonances associated with the bridging hydrides in the ^{1}H NMR spectrum of complexes **1a–c** appear as completely symmetrical and nearly identical patterns due to equivalent coupling to all four phosphines and both rhodium centers; therefore, there is a rapid exchange process operative. Fragmentation yielding mononuclear species can be ruled out as a mechanism for exchanging the hydrides and phosphines on the basis of the binuclearity of these complexes in solution (vide supra) and the absence of crossover product when solutions of $[(dippp)Rh]_2(\mu\text{-}H)_2(\mu\text{-}ZnCH_2Ph)_2$, **1a**, and $[(dippp)Rh]_2(\mu\text{-}H)_2(\mu\text{-}ZnC_5H_5)_2$, **1c**, are allowed to mix.

In previous work,[34] the tetrahydride binuclear rhodium complex $[(dippp)RhH_2]_2$ (V) shows the hydrides as a single resonance in the ^{1}H NMR spectrum at room temperature due to a rapid exchange process; a bridge-to-terminal exchange has been proposed to account for the hydride equivalency in the high temperature limit.[35] However, the exchange process could be "frozen-out" at −80 °C and the various inequivalent hydrides observed in the ^{1}H NMR spectrum. The ^{31}P{^{1}H} NMR spectrum of compound V at −80 °C revealed inequivalent phosphines and phosphorus–rhodium coupling constants ($^1J_{\mathrm{Rh(I),P}}$ = 167.3 Hz and $^1J_{\mathrm{Rh(III),P}}$ = 105.8 Hz) attributable[36,37] to a formally Rh(I)–Rh(III) complex.

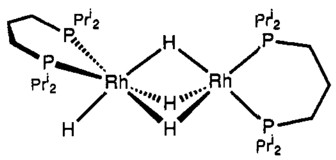

V

The main difference between the organozinc bridged complexes **1a–d** and complex V is the presence of the two organozinc moieties and two hydrides instead of four hydrides. A direct comparison of the solid-state structure of [(dippp)Rh]$_2$(μ-H)$_2$(μ-ZnC$_5$H$_5$)$_2$, **1c**, and structure V above reveals some interesting features. The bridging hydride, H(2), previously corresponding to the terminal hydride shown in the structure of compound V, has adopted a bridging position between Rh(1) and Zn(2). Interestingly, Zn(1) and Zn(2) are both statistically closer to Rh(2) than to Rh(1), thus a Rh(I)–Rh(III) framework, as in complex V, is likely present. It is conceivable that the zinc centers aid in the exchange of the hydrides from one rhodium center to the other in complexes **1a–c**. In order to account for the equivalency of the phosphines a *butterfly* motion of the bridging organozinc moieties above and below the rhodium–diphosphine plane concomitant with hydride exchange is advanced. However, it should be noted that because we were unable to observe any decoalescence to give some information on the fluxional process, the proposed exchange mechanism is purely speculative.

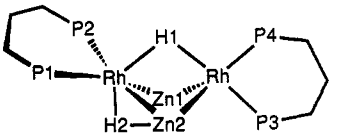

1c

Reactions with Other ZnR$_2$ and MgR$_2$ Compounds. The binuclear rhodium hydride dimer [(dippp)Rh]$_2$(μ-H)$_2$, I, also reacts with dialkylzinc reagents such as ZnEt$_2$, ZnMe$_2$, Zn(CH$_2$Bu^t)$_2$, and Zn(HC=CMe$_2$)$_2$ to give the corresponding tetranuclear derivatives, as evidenced by ^{31}P{^{1}H} NMR spectroscopy; however, the associated mononuclear Rh(I) species generated are apparently unstable and this has made the isolation of the tetranuclear complexes impossible.

As described above for the zinc reagents, the reaction of 1 equiv of dibenzylmagnesium bis(tetrahydrofuran), Mg(CH$_2$Ph)$_2$(THF)$_2$,[23] with I was found to generate two compounds by ^{31}P{^{1}H} NMR spectroscopy (eq 4). One of the compounds was identified as the η^3-benzyl derivative (dippp)Rh(η^3-CH$_2$Ph), **2a**, by ^{1}H and ^{31}P{^{1}H} NMR spectroscopy. The other complex (dippp)Rh(μ-H)$_2$(MgCH$_2$Ph) (**3**), which was isolated as a yellow powder, did not resemble the Rh$_2$Zn$_2$ tetranuclear complexes described above, as evidenced by solution spectral measurements, in particular, the ^{1}H NMR spectrum of complex **3** shows a second-order hydride pattern at −6.64 ppm and a simple symmetrical doublet ($^1J_{\mathrm{P,Rh}}$ = 124 Hz) in the ^{31}P{^{1}H} NMR spectrum. The thermal sensitivity of this complex thwarted all attempts to obtain accurate microanalytical data; however, the compound is stable at −40 °C for months. Surprisingly, there was no reaction between I and MgCp$_2$ even after prolonged heating.

$$[(\mathrm{dippp})\mathrm{Rh}]_2(\mu\text{-})_2 + \mathrm{Mg(CH_2Ph)_2(THF)_2} \xrightarrow{-^1/_2\mathrm{H_2}} \underset{\mathbf{3}}{(\mathrm{dippp})\mathrm{Rh}(\mu\text{-H})_2(\mathrm{MgCH_2Ph})} + \underset{\mathbf{2a}}{(\mathrm{dippp})\mathrm{Rh}(\eta^3\text{-CH_2Ph})} \quad (4)$$

Isolated (dippp)Rh(μ-H)$_2$(MgCH$_2$Ph), **3**, reacts reversibly with 1 atm of dihydrogen to give a single product (**4**), as evidenced by ^{31}P{^{1}H} NMR spectroscopy; specifically, a new resonance is observed at 55.1 ppm, which shows a reduced $^1J_{\mathrm{P,Rh}}$ value of 94 Hz indicative of a Rh(III) species.[36,37] The ^{1}H NMR spectrum of compound **4** shows a ten-line pattern at −9.18 ppm, which is attributable to two terminally bound hydrides on rhodium (Figure 6a). A second hydride resonance at −10.28 ppm, which also integrated to two protons appears as a second-order multiplet. Only one benzyl ligand was present with respect to integration of the diphosphine ligand.

The ^{1}H{^{31}P} NMR spectrum of **4** revealed the multiplicity of the two hydride patterns. Decoupling of the ^{31}P nuclei in **4** reduces the terminal hydride pattern to a simple doublet of triplets due to coupling to ^{103}Rh and coupling to two equivalent bridging hydrides (Figure 6b). The pattern for the bridging hydrides is reduced from a second-order pattern to a simple doublet of triplets because of coupling to ^{103}Rh and coupling to two equivalent terminal hydrides. The proposed structure of **4**, [(dippp)RhH$_2$](μ-H)$_2$(MgCH$_2$Ph), is shown below.

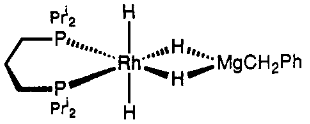

4

Mechanism of Formation of [(dippp)Rh]$_2$(μ-H)$_2$(μ-ZnR)$_2$. The reaction between Zn(CH$_2$Ph)$_2$ and [(dippp)Rh]$_2$(μ-H)$_2$ is complete within a few seconds at −80 °C, and therefore a detailed kinetic analysis was not attempted; however product analysis was quite useful in formulating a mechanism. The reaction of Zn(CH$_2$Ph)$_2$ and [(dippp)Rh]$_2$(μ-D)$_2$[34] (I-d_2) resulted in the formation of [(dippp)Rh]$_2$(μ-D)$_2$(μ-ZnCH$_2$Ph)$_2$ (**1a**-d_2) and (dippp)Rh(η^3-CH$_2$Ph) only, with no detectable deuterium incorporation in the η^3-benzyl moiety or anywhere else, as measured by ^{2}H{^{1}H} NMR spectroscopy. A possible mechanism consistent with the deuterium labeling experiment and product analysis is shown in Scheme II.

Formal oxidative addition of the Zn–C bond[38] across the rhodium hydride core of [(dippp)Rh]$_2$(μ-H)$_2$ would generate the trimetallic derivative A; upon asymmetric cleavage of A, the Rh(III) fragment B and the Rh(I) fragment C would be generated. Dimerization of B followed by (or concomitant with) loss of H$_2$ completes

---

(37) Meek, D. W.; Mazanec, T. J. *Acc. Chem. Res.* **1981**, *14*, 266.

(38) Budzelaar, P. H. M.; Boersma, J.; van der Kerk, G. J. M.; Spek, A. L.; Duisenberg, A. J. M. *Organometallics* **1985**, *4*, 680.

Figure 6. (a) 500-MHz ^1H NMR spectrum of the hydride region of [(dippp)Rh](μ-H)$_2$($MgCH_2Ph$) (4). (b) $^1H\{^{31}P\}$ NMR spectrum of the hydride region of 4.

the formation of complex **1a**. Alternatively, fragment B could lose H_2 to give a monomeric rhodium–zinc benzyl complex and then recombine with another fragment of B to give the tetranuclear derivative **1a**. The Rh(I) fragment C must isomerize to the η^3 form, which presumably stabilizes an otherwise reactive Rh(I) 14-electron complex. In a similar fashion the dialkylzinc reagents $Zn(C_5H_5)_2$ and $Zn(C_3H_5)_2$ react to give the observed products. It is believed that this sequence of reactions is general for all dialkylzinc reagents including $ZnEt_2$, $ZnMe_2$, $Zn(CH_2Bu^t)_2$, and $Zn(HC{=}CMe_2)_2$.

Crossover Experiments. A key intermediate in the mechanism outlined in Scheme II is species B, (dippp)-$RhH_2(ZnCH_2Ph)$, which is formed by the fragmentation of A. Given the presumed high reactivity of such an intermediate and out inability to observe such a species by low temperature $^{31}P\{^1H\}$ NMR spectroscopy, a crossover experiment was devised in order to demonstrate its existence. The goal was to have fragment B recombine with a similar, but different, fragment and observe the *unsymmetrical* derivative by $^{31}P\{^1H\}$ and ^1H NMR spectroscopy. Replacement of the diphosphine having a three carbon atom backbone (dippp) with the two carbon analogue, $Pr^i_2PCH_2CH_2PPr^i_2$ (dippe), results in a subtle chemical change; however, the spectroscopic difference is large since the *dippp* (six-membered chelate ring) and the *dippe* (five-membered chelate ring) phosphorus-31 resonances[39] are normally separated by 30–60 ppm.

Scheme II

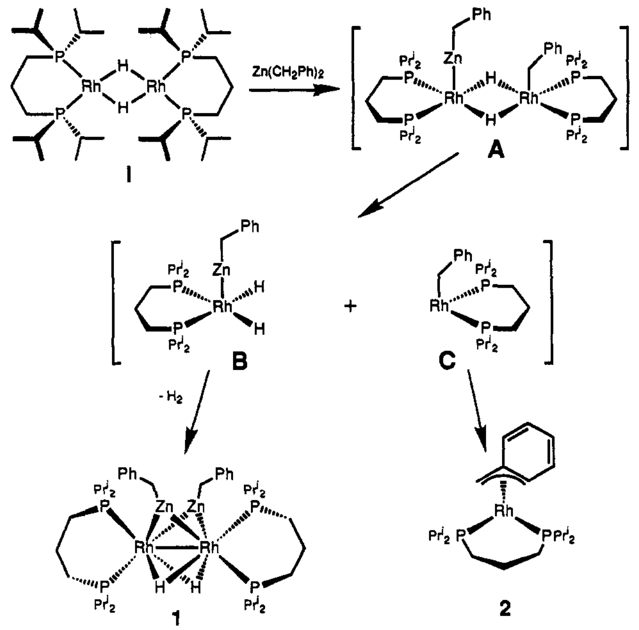

The first crossover experiment was performed by the addition of 1 equiv of $Zn(CH_2Ph)_2$ to a mixture of $^1/_2$ equiv of [(dippp)Rh]$_2$(μ-H)$_2$, I, and $^1/_2$ equiv of [(dippe)Rh]$_2$(μ-H)$_2$, II. Besides the formation of the expected symmetrical products, a new compound was present, as shown by $^{31}P\{^1H\}$ NMR spectroscopy. The new species showed a doublet in the "dippe region" at 104.4 ppm and a second doublet in the "dippp region" at 50.4 ppm. Closer inspection of the two new doublets revealed identical secondary couplings of 4.9 Hz, which can be attributed to long range three bond P_{dippp}–P_{dippe} coupling across the newly formed dippp–dippe dimer [(dippp)Rh](μ-H)$_2$(μ-$ZnCH_2Ph$)$_2$[Rh(dippe)] (**1e**). Further evidence for this new mixed diphosphine complex comes from the ^1H NMR of the mixture which shows a new hydride multiplet at −8.31 ppm and a third benzylic proton resonance ($ZnCH_2Ph$) at 2.12 ppm. We were unable to separate the three species (i.e. **1a**, **1b**, and **1c**) by any means.

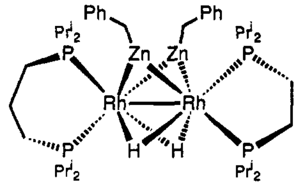

1e

As mentioned above, the formation of the tetranuclear complexes **1a–e** likely proceeds through an intermediate such as (dippp)$RhH_2(ZnR)$ (B). The loss of H_2 from this fragment occurs either before or concomitant with the dimerization process. If H_2 is lost from the dimeric intermediate, then addition of dihydrogen to complexes

---

[39] Garrou, P. E. *Chem. Rev.* **1981**, *81*, 229.

such as $[(dippp)Rh]_2(\mu\text{-H})_2(\mu\text{-ZnCH}_2\text{Ph})_2$, **1a**, may yield this intermediate. The addition of excess (4 atm) dihydrogen to complexes **1a** or **1c** in a sealed NMR tube yields new complexes, as evidenced by $^{31}P\{^1H\}$ NMR spectroscopy (eq 5). The temperature invariant $^{31}P\{^1H\}$ NMR spectra

$$\begin{array}{l} [(dippp)Rh]_2(\mu\text{-H})_2(\mu\text{-ZnR})_2 \overset{4\ \text{atm of H}_2}{\rightleftharpoons} \\ \quad \mathbf{1a},\ R = CH_2Ph \\ \quad \mathbf{1c},\ R = C_5H_5 \\ \qquad\qquad [(dippp)RhH_2(ZnR)]_x \quad (5) \\ \qquad\qquad\quad \mathbf{5},\ R = CH_2Ph \\ \qquad\qquad\quad \mathbf{6},\ R = C_5H_5 \end{array}$$

of complexes $[(dippp)RhH_2(ZnCH_2Ph)]_x$, **5**, and $[(dippp)RhH_2(ZnC_5H_5)]_x$, **6**, display reduced $^1J_{P,Rh}$ values of 103 and 106 Hz, respectively, indicating the presence of a Rh(III) species.[36,37] Complexes **5** and **6** readily lose H_2 when exposed to vacuum and revert back to the dehydrogenated tetranuclear precursors **1a** and **1c**, thus the nuclearity of the complexes could not be unambiguously determined. However, they are most likely tetranuclear species and not simply the bimetallic species $(dippp)RhH_2(ZnR)$ (vide infra).

Interestingly, a solution of $[(dippp)Rh]_2(\mu\text{-H})_2(\mu\text{-ZnCH}_2\text{Ph})_2$, **1a**, and $[(dippe)Rh]_2(\mu\text{-H})_2(\mu\text{-ZnCH}_2\text{Ph})_2$, **1b**, when exposed to dihydrogen (4 atm) for 5 min followed by dihydrogenation under vacuum yields about 10% of the *crossover product* $[(dippp)Rh](\mu\text{-H})_2(\mu\text{-ZnCH}_2\text{Ph})_2[Rh(dippe)]$, **1e**. In the absence of dihydrogen this same solution monitored 24 h later showed no further crossover. Exposure of the same solution again to 4 atm of dihydrogen followed by heating to 50 °C for 10 min showed, after removing the dihydrogen under vacuum, approximately 25% crossover. On the basis of this result it is proposed that the hydrogenated intermediate is a dirhodium species but it is in equilibrium with the monomeric Rh(III) complex B described in Scheme II. It is also significant that the tetranuclear species **1a–d** do not fragment in the absence of H_2.

Summary

It has been found that the coordinatively unsaturated binuclear hydride dimers $[P_2Rh]_2(\mu\text{-H})_2$ (P_2 = dippp, dippe) react with the dialkylzinc species, ZnR_2 (R = CH_2Ph, C_5H_5, C_3H_5), to generate a mixture of two products: a mononuclear Rh(I) derivative P_2RhR and a tetranuclear complex of the general formula $[P_2Rh]_2(\mu\text{-H})_2(\mu\text{-ZnR})_2$. This reaction appears to be general, although the isolation of the products is facilitated when the mononuclear Rh(I) derivative is stable. The tetranuclear complexes react reversibly with dihydrogen to give polyhydride species that are in equilibrium with monomeric Rh(III) complexes of the form P_2RhH_2ZnR, as evidenced by crossover experiments. A mechanism for the reaction of ZnR_2 with the hydride dimers I and II based on product analysis and two separate crossover experiments has been proposed that involves fragmentation and recombination of rhodium–zinc fragments. The reaction of dibenzylmagnesium, $Mg(CH_2Ph)_2$, with $[(dippp)Rh]_2(\mu\text{-H})_2$ is similar in that the same mononuclear Rh(I) species is formed, namely $(dippp)Rh(\eta^3\text{-CH}_2\text{Ph})$; however, the second product is proposed to be the heterobimetallic complex $(dippp)Rh(\mu\text{-H})_2MgCH_2Ph$, which does not dimerize. One possible explanation for the difference in structures of the zinc and magnesium adducts might be that the more electropositive magnesium stabilizes the square planar anionic unit, $[(dippp)RhH_2]^-$, which would not be expected to dimerize simply on electrostatic grounds; the more electronegative zinc atom engages in a more covalent interaction which has less difficulty dimerizing and losing hydrogen. The heterobimetallic magnesium complex reacts reversibly with dihydrogen to yield the rhodium–magnesium tetrahydride derivative, $(dippp)RhH_2(\mu\text{-H})_2MgCH_2Ph$.

Future studies will center around the reaction of ZnH_2 and MgH_2 with $[(dippp)Rh]_2(\mu\text{-H})_2$ since these reactions may be promising in terms of preparing complexes which contain electropositive metals stabilized by the anion $(P_2RhH_2)^-$. The observation that hydrides can indeed interact in a bridging fashion with electropositive metals such as zinc and magnesium suggests that such high nuclearity species may be useful *models* for hydrogen storage materials.

Experimental Section

General Details. All manipulations were performed under prepurified nitrogen in a Vacuum Atmospheres HE-553-2 glovebox equipped with a MO-40-2H purifier or in standard Schlenk-type glassware on a vacuum line. Toluene, hexanes, and THF were predried over CaH_2 for 24 h and then refluxed over sodium–benzophenone ketyl followed by distillation under argon. Deuterated benzene (C_6D_6) and toluene (C_7D_8) were dried over activated 4-Å molecular sieves, vacuum transferred, and degassed three times prior to use. Hydrogen gas was purified by passing through a column packed with activated molecular sieves and MnO. Microanalyses of all air- and moisture-sensitive compounds were performed by Mr. Peter Borda of this department.

All NMR spectra were recorded at room temperature (20 °C) unless otherwise indicated. ^1H NMR spectra were recorded on either a Varian XL-300 (299.94 MHz) or a Bruker WH-400 (400.00 MHz) spectrometer and referenced to C_6D_5H or $C_6D_5CD_2H$ set at 7.15 and 2.09 ppm, respectively. $^{31}P\{^1H\}$ NMR spectra were recorded on a Varian XL-300 spectrometer (121.42 MHz) and referenced to external $P(OMe)_3$ set at 141.00 ppm relative to 85% H_3PO_4. $^1H\{^{31}P\}$ NMR were recorded on a Bruker AMX-500 (500.13 MHz) spectrometer.

Syntheses. Hydrated rhodium trichloride, $RhCl_3(H_2O)_x$, was obtained from Johnson-Matthey and used to prepare $[(\eta^4\text{-C}_8H_{12})Rh]_2(\mu\text{-Cl})_2$.[40] 1,3-Bis(diisopropylphosphino)propane (dippp),[41] 2-bis(diisopropylphosphino)ethane (dippe),[42] $[(dippp)Rh]_2(\mu\text{-H})_2$,[34] and $[(dippe)Rh]_2(\mu\text{-H})_2$[42] were prepared by literature methods. $[(dippp)Rh]_2(\mu\text{-Cl})_2$ was prepared[20] by adding 2 equiv of dippp to $[(\eta^4\text{-C}_8H_{12})Rh]_2(\mu\text{-Cl})_2$. $Zn(CH_2Ph)_2$,[23] $Mg(CH_2Ph)_2(THF)_2$,[23] and $Zn(C_3H_5)_2$[33] were prepared by literature methods. $Zn(C_5H_5)_2$ was prepared[26] using a modification of the procedure outlined in the literature.[43] The compounds $(dippp)Rh(\eta^3\text{-C}_3H_5)$,[35] $(dippp)Rh(\eta^3\text{-CH}_2\text{Ph})$,[24] and $(dippe)Rh(\eta^3\text{-CH}_2\text{Ph})$[24] have been reported.

$[(dippp)Rh]_2(\mu\text{-H})_2(\mu\text{-ZnCH}_2\text{Ph})_2$ (1a). To a stirred green toluene solution (25 mL) of $[(dippp)Rh]_2(\mu\text{-H})_2$ (203 mg, 0.266 mmol) was added dropwise a toluene solution (5 mL) of $Zn(CH_2Ph)_2$ (66 mg, 0.27 mmol). The color of the solution turned orange-red instantly. The solution was filtered through Celite and concentrated to 15 mL. Cooling the solution to −40 °C for 24 h yielded 118 mg of red crystalline **1a** (83% based on rhodium). Anal. Calcd for $C_{44}H_{84}P_4Rh_2Zn_2$: C, 49.22; H, 7.88. Found: C, 49.07; H, 7.73. ^1H NMR (C_6D_6, δ, ppm): 7.25–6.92 (m, phenyl

---

(40) Chatt, J.; Venanzi, L. M. *J. Chem. Soc.* **1957**, 4753.

(41) Tani, K.; Tanigawa, E.; Tatsubo, Y.; Otsuka, S. *J. Organomet. Chem.* **1985**, *279*, 87.

(42) Fryzuk, M. D.; Jones, T.; Einstein, F. W. B. *Organometallics* **1984**, *3*, 185.

(43) Lorberth, J. *J. Organomet. Chem.* **1969**, *19*, 189.

Table I. Crystallographic Data[a]

formula	$C_{44}H_{84}P_4Rh_2Zn_2$ (**1a**)	$C_{40}H_{80}P_4Rh_2Zn_2{\cdot}C_7H_8$ (**1c**)
fw	1073.61	1113.68
cryst syst	monoclinic	monoclinic
space group	$C2/c$	$P2_1/n$
a, Å	19.608(7)	12.050(6)
b, Å	12.891(6)	35.230(4)
c, Å	22.847(6)	12.414(2)
α, deg		
β, deg	120.02(2)	97.84(3)
γ, deg		
V, Å^3	5001(3)	5221(3)
Z	4	4
ρ_{calc}, g/cm^3	1.426	1.417
$F(000)$	2232	2320
μ(Mo Kα), cm^{-1}	17.65	16.93
cryst size, mm	0.25 × 0.30 × 0.34	0.20 × 0.30 × 0.40
transm factors	0.84–1.00	0.90–1.00
scan type	ω–2θ	ω
scan range, deg in ω	$1.05 + 0.35 \tan\theta$	$1.13 + 0.35 \tan\theta$
scan rate, deg/min	32	16
data collcd	$+h,\pm k,\pm l$	$+h,+k,\pm l$
$2\theta_{max}$, deg	60	55
cryst decay, %	negligible	2.40
p factor in $\sigma(I)$ calcn	0.03	0.01
total no. of reflns	6185	12 761
no. of unique reflns	6009	12 197
R_{merge}	0.032	0.036
no. of reflns with $I \geq 3\sigma(I)$	2773	6143
variables	239	505
R	0.044	0.032
R_w	0.048	0.029
gof	1.64	1.52
max Δ/σ (final cycle)	0.03	0.05
residual density e/Å^3	−1.19 to +1.46	−0.53 to +0.48

[a] Temperature 294 K, function minimized $\sum w(|F_o| - |F_c|)^2$ where $w = 4F_o^2/\sigma^2(R_o^2)$, $R = \sum||F_o| - |F_c||/\sum|F_o|$, $R_w = (\sum w(|F_o| - |F_c|)^2/\sum w|F_o|^2)^{1/2}$, and gof $= [\sum(|F_o| - |F_c|)^2/(m - n)]^{1/2}$. Values given for R, R_w, and gof are based on those reflections with $I \geq 3\sigma(I)$, Rigaku AFC6S diffractometer, Mo Kα radiation (λ = 0.710 69 Å), graphite monochromator, takeoff angle 6.0°, aperture 6.0 × 6.0 mm at a distance of 285 mm from the crystal, stationary background counts at each end of the scan (scan/background time ratio 2:1, up to 8 rescans), $\sigma^2(F^2) = [S^2(C + 4B) + (pF^2)^2]/Lp^2$ (S = scan rate, C = scan count, B = normalized background count).

Table II. Final Atomic Coordinates (Fractional) and B(eq) Values (Å^2) for $[(dippp)Rh]_2(\mu\text{-}H)_2(\mu\text{-}ZnCH_2Ph)_2$, 1a

atom	x	y	z	B(eq)
Rh(1)	0.42356(3)	0.55656(4)	0.19637(3)	3.03(2)
Zn(1)	0.46718(5)	0.44026(7)	0.29722(5)	4.60(4)
P(1)	0.3368(1)	0.4812(1)	0.0977(1)	3.56(7)
P(2)	0.3415(1)	0.6827(2)	0.1928(1)	3.53(7)
C(1)	0.2417(4)	0.5461(7)	0.0452(4)	5.4(3)
C(2)	0.2039(5)	0.5976(8)	0.0805(5)	7.8(5)
C(3)	0.2423(4)	0.6955(6)	0.1179(4)	4.8(3)
C(4)	0.3025(4)	0.3469(6)	0.0990(4)	4.4(3)
C(5)	0.3729(4)	0.4678(6)	0.0364(4)	4.6(3)
C(6)	0.3178(4)	0.6905(6)	0.2615(4)	4.8(4)
C(7)	0.3822(4)	0.8133(6)	0.1953(4)	4.8(3)
C(8)	0.2581(5)	0.3416(7)	0.1370(5)	6.3(4)
C(9)	0.3683(5)	0.2675()	0.1257(5)	5.9(4)
C(10)	0.4024(6)	0.5709(8)	0.0262(4)	7.0(5)
C(11)	0.3157(6)	0.4164(8)	−0.0317(4)	7.2(5)
C(12)	0.2751(5)	0.5933(7)	0.2630(5)	5.9(4)
C(13)	0.3905(5)	0.7107(8)	0.3302(4)	6.5(5)
C(14)	0.4023(5)	0.8259(7)	0.1399(5)	6.5(4)
C(15)	0.3331(6)	0.9051(7)	0.1960(6)	7.4(5)
C(16)	0.4117(5)	0.3575(7)	0.3362(5)	6.9(5)
C(17)	0.4467(4)	0.2574(7)	0.3695(5)	4.6(4)
C(18)	0.4400(5)	0.1720(9)	0.3334(5)	6.7(5)
C(19)	0.4723(7)	0.0808(9)	0.3621(7)	8.5(6)
C(20)	0.5137(7)	0.071(1)	0.4293(7)	8.2(6)
C(21)	0.5229(6)	0.150(1)	0.4706(5)	7.4(5)
C(22)	0.4878(5)	0.2472(8)	0.4401(5)	6.3(5)
H(1)	0.528(6)	0.594(7)	0.237(6)	12(3)

Table III. Selected Bond Lengths (Å) and Angles (deg) for $[(dippp)Rh]_2(\mu\text{-}H)_2(\mu\text{-}ZnCH_2Ph)_2$, 1a

	Bond Lengths		
Rh(1)–Rh(1)*	2.764(1)	Rh(1)–Zn(1)	2.513(1)
Rh(1)*–Zn(1)	2.558(1)	Rh(1)–P(1)	2.255(2)
Rh(1)–P(2)	2.261(2)	Rh(1)–H(1)	1.8(1)
Rh(1)*–H(1)	1.4(1)	Zn(1)–C(16)	2.020(8)
	Bond Angles		
P(1)–Rh(1)–P(2)	96.12(7)	P(1)–Rh(1)–H(1)	136(3)
P(1)–Rh(1)–Zn(1)	113.58(6)	P(1)–Rh(1)–H(1)*	171(3)
Rh(1)–Zn(1)–Rh(1)*	66.05(4)	Rh(1)–H(1)–Rh(1)*	116(5)
Zn(1)–Rh(1)–Zn(1)*	72.94(4)	P(2)–Rh(1)–Zn(1)*	169.86(6)
P(2)–Rh(1)–Zn(1)	111.82(6)	P(1)–Rh(1)–Zn(1)*	89.77(6)

protons, 10H), 2.34 (s, CH_2Ph, 4H), 1.69 (d of sept, $PCH(CH_3)_2$, 8H, $^2J_{H,P}$ = 7.0 Hz, $^3J_{H,H}$ = 7.0 Hz), 1.17 (m, PCH_2 and PCH_2CH_2, 12H), 1.12 (dd, $PCH(CH_3)_2$, 24H, $^3J_{H,P}$ = 13.1 Hz, $^3J_{H,H}$ = 7.0 Hz), 0.95 (dd, $PCH(CH_3)_2$, 24H, $^3J_{H,P}$ = 13.3 Hz, $^3J_{H,H}$ = 7.0 Hz), −9.37 (t of quintet, Rh–*H*, 2H, $^2J_{H,P}$ = 20 Hz, $^1J_{H,P}$ = 14 Hz). $^{31}P\{^1H\}$ NMR (C_6D_6, δ, ppm): 46.7 (d of m, $^1J_{P,Rh}$ = 154 Hz).

$[(dippe)Rh]_2(\mu\text{-}H)_2(\mu\text{-}ZnCH_2Ph)_2$ (1b). The synthesis of compound **1b** is identical to the procedure outlined for complex **1a**. $[(dippe)Rh]_2(\mu\text{-}H)_2$ (86 mg, 0.12 mmol) and $Zn(CH_2Ph)_2$ (30 mg, 0.12 mmol) gave 43 mg of red crystalline **1b** (71% based on rhodium). Anal. Calcd for $C_{42}H_{80}P_4Rh_2Zn_2$: C, 48.25; H, 7.71. Found: C, 48.24; H, 7.80. ^1H NMR (C_6D_6, δ, ppm): 7.28–6.92 (m, phenyl protons, 10H), 2.22 (s, CH_2Ph, 4H), 1.78 (d of sept, $PCH(CH_3)_2$, 8H, $^2J_{H,P}$ = 7.2 Hz, $^3J_{H,H}$ = 7.2 Hz), 1.16 (d of m, PCH_2, 8H, $^3J_{H,P}$ = 13.2 Hz), 1.15 (dd, $PCH(CH_3)_2$, 24H, $^3J_{H,P}$ = 15.6 Hz, $^3J_{H,H}$ = 7.2 Hz), 0.88 (dd, $PCH(CH_3)_2$, 24H, $^3J_{H,P}$ = 12.6 Hz, $^3J_{H,H}$ = 7.2 Hz), −7.84 (t of quintet, Rh–*H*, 2H, $^2J_{H,P}$ = 21.4 Hz, $^1J_{H,Rh}$ = 19.2 Hz). $^{31}P\{^1H\}$ NMR (C_6D_6, δ, ppm): 107.7 (d of m, $^1J_{P,Rh}$ = 165 Hz).

$[(dippp)Rh]_2(\mu\text{-}H)_2(\mu\text{-}ZnC_5H_5)_2$ (1c). To a stirred green THF solution (25 mL) of $[(dippp)Rh]_2(\mu\text{-}H)_2$ (623 mg, 0.819 mmol) was added dropwise a THF solution (5 mL) of $Zn(C_5H_5)_2$ (178 mg, 0.910 mmol) (10% excess). The color of the solution turned orange-red instantly. The THF was removed under vacuum and the product extracted with toluene (25 mL). The solution was filtered through Celite and concentrated to 15 mL. Cooling the solution to −40 °C for 24 h yielded 330 mg of orange crystalline **1c** (79% based on rhodium). Anal. Calcd for $C_{40}H_{80}P_4Rh_2Zn_2$: C, 47.03; H, 7.89. Found: C, 46.84; H, 8.02. ^1H NMR (C_7D_8, δ, ppm): 6.48 (s, C_5H_5, 10H), 1.90 (d of sept, $PCH(CH_3)_2$, 8H, $^2J_{H,P}$ = 7.1 Hz, $^3J_{H,H}$ = 7.1 Hz), 1.69 (m, PCH_2 and PCH_2CH_2, 12H), 1.19 (dd, $PCH(CH_3)_2$, 24H, $^3J_{H,P}$ = 12.9 Hz, $^3J_{H,H}$ = 7.1 Hz), 1.12 (dd, $PCH(CH_3)_2$, 24H, $^3J_{H,P}$ = 13.1 Hz, $^3J_{H,H}$ = 7.1 Hz), −12.12 (t of quintet, Rh–*H*, 2H, $^2J_{H,P}$ = 14.7 Hz, $^1J_{H,Rh}$ = 14.7 Hz). $^{31}P\{^1H\}$ NMR (C_7D_8, δ, ppm): 44.7 (d of m, $^1J_{P,Rh}$ = 151 Hz).

$[(dippp)Rh]_2(\mu\text{-}H)_2(\mu\text{-}ZnC_3H_5)_2$ (1d). To a stirred green THF solution (25 mL) of $[(dippp)Rh]_2(\mu\text{-}H)_2$ (224 mg, 0.294 mmol) was added dropwise a THF solution (5 mL) of $Zn(C_3H_5)_2$ (46 mg, 0.31 mmol) (10% excess). The color of the solution turned orange-red instantly. The THF was removed under vacuum and the mixture dissolved in hexanes (20 mL). Concentration of the sample to 10 mL followed by cooling yielded 81 mg of red crstalline **1d** (57%). The reaction is quantitative by $^{31}P\{^1H\}$ NMR spectroscopy. The product was slightly contaminated with $(dippp)Rh(\eta^3\text{-}C_3H_5)$ (**2d**); thus accurate microanalysis could not obtained. ^1H NMR (C_6D_6, δ, ppm): 6.54 (quintet, H_c of allyl, 2H, $^3J_{H,H}$ = 11 Hz), 3.58 (d, $H_{syn,anti}$ of allyl, 8H, $^3J_{H,H}$ = 11 Hz), 1.88 (d of sept, $PCH(CH_3)_2$, 8H), 1.73 (m, PCH_2 and PCH_2CH_2, 12H), 1.09 (d of d, $PCH(CH_3)_2$, 24H), 1.01 (d of d, $PCH(CH_3)_2$, 24H), −9.34 (t of quintets, Rh–*H*, 2H, $^2J_{H,P}$ = 21 Hz, $^1J_{H,Rh}$ = 18 Hz). $^{31}P\{^1H\}$ NMR (C_6D_6, δ, ppm): 47.4 (d of m, $^1J_{P,Rh}$ = 155 Hz).

$(dippp)Rh(\eta^5\text{-}C_5H_5)$ (2c). Compound **2c** was observed in the crude reaction mixture of $[(dippp)Rh]_2(\mu\text{-}H)_2$ and $Zn(C_5H_5)_2$ and was synthesized directly from $[(dippp)Rh]_2(\mu\text{-}Cl)_2$ and $Zn(C_5H_5)_2$. To a stirred toluene suspension (25 mL) of $[(dippp)Rh]_2(\mu\text{-}Cl)_2$ (201 mg, 0.242 mmol) was added $Zn(C_5H_5)_2$ (49 mg, 0.25 mmol) as a solid. The mixture was stirred for 24 h as the solution turned dark orange. The toluene was removed under vacuum and the

Table IV. Final Atomic Coordinates (Fractional) and B_{eq} Values (Å^2)^a for $[(\text{dippp})\text{Rh}]_2(\mu\text{-H})_2(\mu\text{-ZnC}_5\text{H}_5)_2$, 1c

atom	*x*	*y*	*z*	B_{eq}	occ
Rh(1)	0.49163(3)	0.154958(9)	0.32386(3)	3.14(1)	
Rh(2)	0.63513(3)	0.110973(9)	0.19497(3)	2.93(1)	
Zn(1)	0.49790(5)	0.15914(1)	0.11474(4)	4.33(3)	
Zn(2)	0.44451(4)	0.09205(1)	0.22042(4)	3.76(2)	
P(1)	0.3473(1)	0.18077(3)	0.3956(1)	4.05(6)	
P(2)	0.6220(1)	0.19856(3)	0.3953(1)	3.87(6)	
P(3)	0.6751(1)	0.09406(3)	0.0264(1)	3.58(5)	
P(4)	0.7361(1)	0.06290(3)	0.2900(1)	3.46(5)	
C(1)	0.3793(4)	0.2182(1)	0.4981(4)	5.8(3)	
C(2)	0.4582(5)	0.2483(2)	0.4674(5)	7.3(3)	
C(3)	0.5805(4)	0.2369(1)	0.4841(4)	5.4(3)	
C(4)	0.2731(4)	0.1453(1)	0.4701(4)	4.9(3)	
C(5)	0.2365(5)	0.2032(2)	0.2979(6)	7.5(4)	
C(6)	0.7020(5)	0.2275(1)	0.3060(4)	5.7(3)	
C(7)	0.7337(4)	0.1749(1)	0.4898(4)	4.8(2)	
C(8)	0.3574(5)	0.1219(2)	0.5452(4)	6.9(3)	
C(9)	0.1824(5)	0.1605(2)	0.5338(5)	8.7(4)	
C(10)	0.1691(5)	0.1741(2)	0.2248(5)	7.1(3)	
C(11)	0.167(1)	0.2344(3)	0.325(1)	8.1(7)	0.64
C(11A)	0.242(2)	0.2380(6)	0.272(1)	8(1)	0.36
C(12)	0.7773(5)	0.2036(2)	0.2454(5)	7.6(3)	
C(13)	0.6203(6)	0.2514(2)	0.2288(5)	8.3(4)	
C(14)	0.6835(5)	0.1537(2)	0.5771(4)	6.4(3)	
C(15)	0.8315(5)	0.2000(2)	0.5390(5)	7.5(3)	
C(16)	0.7373(4)	0.0467(1)	0.0111(4)	4.6(2)	
C(17)	0.7290(4)	0.0187(1)	0.1029(4)	4.9(2)	
C(18)	0.8037(4)	0.0294(1)	0.2078(4)	4.7(2)	
C(19)	0.5618(4)	0.0935(1)	−0.0913(3)	4.4(2)	
C(20)	0.7829(4)	0.1238(1)	−0.0261(4)	4.4(2)	
C(21)	0.6484(4)	0.0311(1)	0.3650(4)	5.4(3)	
C(22)	0.8555(4)	0.0767(1)	0.3947(4)	4.3(2)	
C(23)	0.4703(5)	0.0653(2)	−0.0724(4)	6.5(3)	
C(24)	0.5974(5)	0.0860(2)	−0.2028(4)	6.6(3)	
C(25)	0.7395(5)	0.1632(2)	−0.0632(4)	6.2(3)	
C(26)	0.8874(4)	0.1280(1)	0.0573(4)	5.7(3)	
C(27)	0.9280(4)	0.1064(2)	0.3502(4)	6.1(3)	
C(28)	0.9292(5)	0.0445(2)	0.4459(4)	6.9(3)	
C(29)	0.6195(4)	0.0498(1)	0.4678(4)	5.7(3)	
C(30)	0.6740(6)	−0.0101(2)	0.3771(5)	9.0(4)	
C(31)	0.3871(6)	0.1984(2)	0.0247(4)	6.4(3)	
C(32)	0.3176(6)	0.1709(2)	−0.0300(6)	7.7(4)	
C(33)	0.3485(7)	0.1655(3)	−0.1309(6)	9.2(5)	
C(34)	0.4347(7)	0.1898(3)	−0.1408(6)	8.9(5)	
C(35)	0.4604(6)	0.2107(2)	−0.0478(6)	7.5(4)	
C(36)	0.3580(4)	0.0397(1)	0.1904(4)	4.5(2)	
C(37)	0.2712(4)	0.0615(1)	0.1317(4)	4.8(2)	
C(38)	0.1950(4)	0.0701(2)	0.2015(5)	5.7(3)	
C(39)	0.2319(5)	0.0547(2)	0.3021(5)	6.1(3)	
C(40)	0.3302(5)	0.0359(1)	0.2971(4)	5.5(3)	
C(41)	1.0040(7)	0.1007(3)	0.7976(7)	8.4(5)	
C(42)	1.0560(5)	0.0814(3)	0.8835(6)	7.9(4)	
C(43)	1.0285(7)	0.0452(3)	0.9008(7)	9.2(5)	
C(44)	0.9473(8)	0.0274(2)	0.8282(9)	9.7(6)	
C(45)	0.8983(7)	0.0459(4)	0.7421(*)	10.8(6)	
C(46)	0.9257(8)	0.0841(3)	0.7256(6)	9.3(5)	
C(47)	1.0284(8)	0.1412(3)	0.7813(7)	12.7(6)	

^{a} $B_{eq} = (8/3)\pi^2\sum\sum U_{ij}a_i^*a_j^*(\mathbf{a}_i\cdot\mathbf{a}_j)$.

Table V. Selected Bond Lengths (Å) and Angles (deg) for $[(\text{dippp})\text{Rh}]_2(\mu\text{-H})_2(\mu\text{-ZnC}_5\text{H}_5)_2$, 1c

Bond Lengths			
Rh(1)–Rh(2)	2.9507(9)	Rh(1)–Zn(1)	2.6115(8)
Rh(1)–Zn(2)	2.5854(7)	Rh(1)–P(1)	2.251(2)
Rh(1)–P(2)	2.288(1)	Rh(2)–Zn(1)	2.4812(9)
Rh(2)–Zn(2)	2.453(1)	Rh(2)–P(3)	2.290(1)
Rh(2)–P(4)	2.313(1)	Zn(1)–Zn(2)	2.8200(8)
Zn(1)–C(31)	2.131(5)	Zn(1)–C(32)	2.656(7)
Zn(1)–C(35)	2.706(6)	Zn(2)–C(36)	2.127(4)
Zn(2)–C(37)	2.471(5)	Zn(2)–C(40)	2.659(5)
Rh(1)–H(2)	1.57	Zn(2)–H(2)	1.66
Rh(1)–H(1)	1.72	Rh(2)–H(1)	1.74
Bond Angles			
P(1)–Rh(1)–P(2)	95.86(5)	P(3)–Rh(2)–P(4)	96.55(5)
Rh(1)–Zn(1)–Rh(2)	71.64(2)	Rh(1)–Zn(2)–Rh(2)	70.76(3)
Zn(1)–Rh(1)–Zn(2)	65.72(2)	Zn(1)–Rh(2)–Zn(2)	69.71(3)
Rh(1)–H(1)–Rh(2)	117.2	Rh(1)–H(2)–Zn(2)	106.1
Zn(1)–Rh(2)–P(4)	168.82(3)	P(3)–Rh(2)–H(1)	174.5

product extracted with hexanes (25 mL). Concentration of the solution to 10 mL followed by cooling for 24 h provided 132 mg of orange crystalline **2c** (71%). ^{1}H NMR (C_6D_6, δ, ppm): 5.32 (s, C_5H_5, 5H), 1.49 (d of sept, $PCH(CH_3)_2$, 4H, $^2J_{H,P}$ = 7.0 Hz, $^3J_{H,H}$ = 7.0 Hz), 1.05 (dd, $PCH(CH_3)_2$, 12H, $^3J_{H,P}$ = 13.4 Hz, $^3J_{H,H}$ = 7.0 Hz), 0.95 (dd, $PCH(CH_3)_2$, 12H, $^3J_{H,P}$ = 12.9 Hz, $^3J_{H,H}$ = 7.0 Hz), 0.84 (m, PCH_2 and PCH_2CH_2, 6H). $^{31}P\{^1H\}$ NMR (C_6D_6, δ, ppm): 59.7 (d, $^1J_{P,Rh}$ = 210 Hz).

$(\text{dippp})\text{Rh}(\mu\text{-H})_2\text{MgCH}_2\text{Ph}$ (3). To a stirred green toluene solution (25 mL) of $[(\text{dippp})\text{Rh}]_2(\mu\text{-H})_2$ (478 mg, 0.630 mmol) was added dropwise a toluene solution (5 mL) of $Mg(CH_2Ph)_2(THF)_2$ (221 mg, 0.631 mmol). The color of the solution turned yellow-orange instantly. The solution was filtered through Celite and the toluene removed under vacuum. The mixture was suspended in hexanes (10 mL) and the product collected on a fine frit to give 141 mg of crude **3** (90%). The product can be recrystallized from toluene/hexanes. ^{1}H NMR (C_7D_8, δ, ppm): 7.25–6.75 (m, phenyl protons, 5H), 2.07 (s, MgC_2Ph, 2H), 1.63 (d of sept, $PCH(CH_3)_2$, 4H, $^2J_{H,P}$ = 14.2 Hz, $^3J_{H,H}$ = 7.1 Hz), 1.21 (m, PCH_2 and PCH_2CH_2, 6H), 1.10 (dd, $PCH(CH_3)_2$, 24H, $^3J_{H,P}$ = 13.8 Hz, $^3J_{H,H}$ = 7.1 Hz), −6.64 (d of d of m, Rh–*H*, 2H, $^2J_{H,P}$ = 63.9 Hz, $^1J_{H,Rh}$ = 29.2 Hz). $^{31}P\{^1H\}$ NMR (C_6D_6, δ, ppm): 44.0 (d, $^1J_{P,Rh}$ = 124 Hz).

Observation of $[(\text{dippp})\text{RhH}_2](\mu\text{-H})_2(\text{MgCH}_2\text{Ph})$ (4). Into a sealable NMR tube was weighed 25 mg of compound **3**, and 0.25 mL of C_7D_8 was added. The sample was degassed three times and cooled to −196 °C and purified dihydrogen introduced. The sample was sealed under H_2 and warmed to room temperature. The initially yellow solution decolorized on warming. The reaction is quantitative by $^{31}P\{^1H\}$ NMR spectroscopy. ^{1}H NMR (C_7D_8, δ, ppm): 7.29 (d, H_{ortho}, 2H, $^3J_{H,H}$ = 7.2 Hz), 7.17 (t, H_{meta}, 2H, $^3J_{H,H}$ = 7.2 Hz), 6.75 (t, H_{para}, 1H, $^3J_{H,H}$ = 7.2 Hz), 2.18 (s, $MgCH_2Ph$, 2H), 1.42 (d of sept, $PCH(CH_3)_2$, 4H, $^2J_{H,P}$ = 14.2 Hz, $^3J_{H,H}$ = 7.1 Hz), 1.21 (m, PCH_2 and PCH_2CH_2, 6H), 1.02 (dd, $PCH(CH_3)_2$, 12H, $^3J_{H,P}$ = 13.9 Hz, $^3J_{H,H}$ = 7.1 Hz), 0.94 (dd, $PCH(CH_3)_2$, 12H, $^3J_{H,P}$ = 13.2 Hz, $^3J_{H,H}$ = 7.1 Hz), −9.18 (m, Rh–*H*, 2H), −10.28 (m, Rh–*H*, 2H). $^1H\{^{31}P\}$ NMR (C_7D_8, δ, ppm): −9.18 (d of t of t, Rh–*H*, 2H, $^2J_{H,H}$ = 7 Hz, $^1J_{H,Rh}$ = 21 Hz, $^2J_{H,P}$ = 14 Hz), −10.28 (d of t, Rh–*H*, 2H, $^2J_{H,H}$ = 7 Hz, $^1J_{H,Rh}$ = 25 Hz). $^{31}P\{^1H\}$ NMR (C_6D_6, δ, ppm): 55.1 (d, $^1J_{P,Rh}$ = 94 Hz).

Observation of $[(\text{dippp})\text{Rh}](\mu\text{-H})_2(\mu\text{-ZnCH}_2\text{Ph})_2[\text{Rh}(\text{dippe})]$ (1e). To a stirred green toluene solution (25 mL) of $[(\text{dippp})\text{Rh}]_2(\mu\text{-H})_2$ (98 mg, 0.13 mmol) and $[(\text{dippe})\text{Rh}]_2(\mu\text{-H})_2$ (95 mg, 0.13 mmol) was added in one portion $Zn(CH_2Ph)_2$ (64 mg, 0.25 mmol). The color of the solution turned orange-red instantly. The solution was filtered through Celite and taken to dryness under vacuum. ^{1}H NMR (C_6D_6, δ, ppm): 2.12 (s, CH_2Ph, 4H), −8.31 (t of quintets, Rh–*H*, 2H, $^2J_{H,P}$ = 20 Hz, $^1J_{H,Rh}$ = 15 Hz), resonances of the phenyl groups and of the diphosphine ligands are obscured by those of compounds **1a** and **1b**. $^{31}P\{^1H\}$ NMR (C_6D_6, δ, ppm): 104.4 (d of d of m, P_{dippe}, $^1J_{P,Rh}$ = 155 Hz, $^3J_{P,P'}$ = 4.9 Hz), 50.4 (d of d of m, P_{dippp}, $^1J_{P,Rh}$ = 155 Hz, $^3J_{P',P}$ = 4.9 Hz).

X-ray Crystallographic Analyses of $[(\text{dippp})\text{Rh}]_2(\mu\text{-H})_2(\mu\text{-ZnCH}_2\text{Ph})_2$ (1a) and $[(\text{dippp})\text{Rh}]_2(\mu\text{-H})_2(\mu\text{-ZnC}_5\text{H}_5)_2\cdot\text{C}_6\text{H}_5\text{CH}_3$ (1c). A summary of the refined cell parameters and relevant information regarding the data collection procedure is provided for compounds **1a** and **1c** in Table I. The final unit-cell parameters were obtained by least squares on the setting angles for 25 reflections with 2θ = 20.1–27.0° for **1a** and 2θ = 30.0–35.8° for **1c**. The intensities of three standard reflections, measured after every 200 reflections, remained constant throughout data collection for compound **1a** and declined by 2.40% for **1c**. A linear correction factor was applied to the data of compound **1c** to account for this phenomenon. The data for compounds **1a** and **1c** were processed and corrected for Lorentz and polarization effects and absorption (empirical, based on azimuthal scans for several reflections).[44]

The structure of compound **1a** was solved by a combination of the Patterson method and direct methods,[45] and the remaining non-hydrogen atoms were obtained from subsequent difference Fourier syntheses. All non-hydrogen atoms including metal hydrides were refined with anisotropic thermal parameters. Hydrogen atoms were fixed in calculated positions (C–H = 0.98 Å). The structure of compound **1c** was solved by direct methods.[45] The asymmetric unit contains one molecule of toluene solvent. One isopropyl group exhibited minor disordering. A 2-fold split-atom model for C(11) was refined. The non-hydrogen atoms were refined anisotropically. Metal hydride atoms were placed in difference map positions but were not refined. The remaining hydrogen atoms were fixed in calculated positions (C–H = 0.98 Å). Final atomic coordinates and equivalent isotropic thermal parameters appear in Tables II and IV for **1a** and **1c**, respectively. Selected bond lengths and bond angles for each of **1a** and **1c** appear in Tables III and V, respectively.

Acknowledgment. Financial support for this work was provided by NSERC of Canada (operating grants to M.D.F. and postgraduate scholarship to D.H.M.). We also thank Johnson-Matthey for the generous loan of $RhCl_3$.

Supplementary Material Available: ORTEP drawings and tables of calculated hydrogen atom positions, anisotropic thermal parameters, all bond lengths and angles, and least squares planes for **1a** and **1c** (25 pages). Ordering information is given on any current masthead page.

OM920441U

---

(44) TEXSAN/TEXRAY structure analysis package which includes versions of the following: DIRDIF, direct methods for difference structures, by P. T. Beurskens; ORFLS, full-matrix least-squares, and ORFFE, function and errors, by W. R. Busing, K. O. Martin, and H. A. Levy; ORTEP II, illustrations, by C. K. Johnson.

(45) Structure solution methods: Calbrese, J. C. PHASE—Patterson Heavy Atom Solution Extractor. Ph.D. Thesis, University of Wisconsin—Madison, 1972.